$NiCo_2O_4$ NANOCHAINS SYNTHESIS WITH EFFECTIVE MICROWAVE ABSORPTION CHARACTERISTICS

Quang Dat Tran[1,*], Tuan Linh Nguyen[1], Van Cuong Nguyen[1]

[1]*Faculty of Physics and Chemical Engineering, Le Quy Don Technical University, Hanoi, Vietnam*

Abstract

Nanochains-like $NiCo_2O_4$ material was synthesized via the hydrothermal method utilizing D-glucose template to facilitate microwave absorption across the frequency range of 2 - 18 GHz. Comprehensive characterization employing various analytical techniques was employed to investigate the structural, microstructural, magnetic, and electromagnetic properties. Leveraging the presence of Oxalic acid and D-Glucose, a nanochain morphology comprising spherical nanoparticles (400 - 600 nm) was achieved. The resultant $NiCo_2O_4$ demonstrated a single-phase structure and exhibited the reflection loss (RL) value lower than -20 dB was up to 5.9 GHz within the Ku (12 - 18 GHz) frequency band, at a matching thickness of 2.0 mm. Remarkably, the optimal reflection loss reached -52.5 dB at 15 GHz for samples with a thickness of 2.0 mm, while the widest effective bandwidth extended up to 14.1 GHz for samples with a thickness of 5.0 mm. The superior microwave absorption performance of the chains-like $NiCo_2O_4$ powders was attributed to the synergistic interplay between their dielectric and magnetic properties, facilitating excellent impedance matching. These results indicate that $NiCo_2O_4$ chains-like powders have great promise as a material for microwave absorption.

Keywords*: $NiCo_2O_4$; porous; hydrothermal; microwave absorption.*

1. Introduction

Electromagnetic properties, encompassing electromagnetic absorption and reflection phenomena, confer upon electromagnetic materials a diverse array of functionalities and significant potential, including energy harvesting, intelligent device applications, anti-radiation measures, and electromagnetic camouflage, among others [1]. Notably, the primary allure of electromagnetic materials lies in their applications concerning electromagnetic absorption and shielding, crucial for safeguarding life and preventing signal interference. Leveraging electromagnetic absorption and reflection characteristics to broaden the multifunctionality of materials represents a promising avenue for

[*] Email: dattq@lqdtu.edu.vn
DOI: 10.56651/lqdtu.jst.v2.n01.769.pce

exploration [2]. Microwave absorbing materials (MAMs) play a pivotal role in shielding equipment against electromagnetic waves by dissipating their energy into heat through dielectric and magnetic loss mechanisms [3]. In recent years, one-dimensional (1D) nanomaterials have garnered considerable attention in the realm of microwave absorption materials, owing to their distinctive attributes such as large specific surface area, pronounced shape anisotropy, and superior electron transport properties. An ideal 1D MAM exhibits robust absorption capabilities, broad effective bandwidth, lightweight construction, and cost-effectiveness [4].

Cobalt oxide-based materials (MCo_2O_4, where M = Ni, Co, Zn, Mn or Fe), characterized by a spinel cubic structure, have emerged as promising candidates for MAMs applications due to their dual magnetic and dielectric properties, environmental benignity, and exceptional chemical stability [5]. Among these cobaltites, $NiCo_2O_4$ stands out for its elevated electrical conductivity and magnetic characteristics, rendering it highly suitable for enhancing microwave absorption performance. $NiCo_2O_4$ can adopt various morphologies such as nanosheets [6], wood-texture column-like formations [7], nanoribbons [8], and flower-like structures [8], primarily attributable to the intrinsic properties of cobalt ion precursors. Morphology plays a crucial role in influencing absorption performance by modulating the propagation path of electromagnetic waves and facilitating multiple scattering within the absorbers [6-10]. Wu et al. found that sphere-like $NiCo_2O_4$ particles have a wider effective absorption bandwidth (EAB) of 6.08 GHz compared to urchin-like microstructures, which have an EAB of 5.84 GHz [6]. In the case of wood-texture column-like $NiCo_2O_4$ formations, Chang et al. found that the effective absorption bandwidth (EAB) was 7.1 GHz, and the best reflection loss was -49.73 dB [7]. By modifying the morphology of $NiCo_2O_4$ to resemble hollow spheres, Qin et al. achieved a stronger absorption (-37.5 dB) and a wider EAB of 5.92 GHz [9]. This was the result of improved impedance matching and increased multiple reflections and scatterings within the hollow spheres. Nevertheless, there has been very little investigation into the periodic architectures of $NiCo_2O_4$ materials for use in microwave absorption applications. Almost no studies in the area of microwave absorption have focused on $NiCo_2O_4$'s chains or tubes structure.

In the present study, the synthesis of nanochains-structured $NiCo_2O_4$ powders was undertaken employing D-glucose as a template during the coprecipitation of cobalt and nickel

oxalates within a hydrothermal synthesis framework [10]. Our investigation revealed that the arrangement of $NiCo_2O_4$ nanoparticles into a chains-like morphology resulted in a significantly expanded effective absorption bandwidth and decreased thickness.

2. Experiment

2.1. Synthesis of $NiCo_2O_4$ material

The synthesis of $NiCo_2O_4$ material involved a hydrothermal reaction followed by calcination. Initially, a solution (solution A) comprising 2 mmol of $Ni(NO_3)_2{\cdot}6H_2O$ and 4 mmol of $Co(NO_3)_2{\cdot}6H_2O$ dissolved in 50 mL of deionized water was prepared. Separately, solution B was prepared by dissolving 20 mmol of $H_2C_2O_4.2H_2O$ in 50 mL of water containing 0.5 g of D-glucose [10]. Solution A was then slowly added dropwise into solution B over a duration of 15 minutes. Following 1 hour of magnetic stirring, the resulting mixtures were transferred into a PTFE-lined autoclave with a capacity of 150 mL. The hydrothermal reaction was conducted at 140°C for 8 hours. Subsequently, the products were obtained by filtration and subjected to multiple washes with water and ethanol after the autoclave had cooled to room temperature. The resulting powder was dried at 60°C for 12 h prior to calcination at 500°C for 5 h [9], with a heating rate of 2°C/min, within an air-controlled environment to obtain the final products.

2.2. Characterization and electromagnetic measurements

The morphologies and crystal structures of the $NiCo_2O_4$ material were examined via scanning electron microscopy (SEM, S4800) and X-ray diffraction (XRD, Bruker D5, utilizing CuK_1 radiation with a wavelength of 1.54056 Å). Magnetic measurements were conducted using a vibrating sample magnetometer (VSM), with a Lakeshore 7400 instrument employed for this purpose. In a standard experiment, the $NiCo_2O_4$ material was mixed with paraffin wax to create the uniform combination. The material was 30% by weight of the entire combination. A toroidal shape with an inner diameter of 3.04 mm and an outer diameter of 7.0 mm was formed by pressing the completed mixes. The Keysight PNA-X N5242A vector network analyzer was used to test the microwave absorption characteristics. Through the use of the transmission line theory, the characteristics of microwave absorption were ascertained. Exact calculations for the reflection loss (RL) were performed using the following equations [11]:

$$RL\,(\mathrm{dB}) = 20.\log\left|\frac{Z_{in}-1}{Z_{in}+1}\right| \tag{1}$$

$$Z_{in} = \sqrt{\frac{\mu_r}{\varepsilon_r}}\tanh\left(j\frac{2\pi fd}{c}\sqrt{\mu_r\varepsilon_r}\right) \tag{2}$$

where Z_{in} represents the input impedance of the absorber, while ε_r and μ_r denote the complex relative permittivity and permeability, respectively. The velocity of electromagnetic waves in vacuum is denoted by *c*, while *f* represents the frequency of the electromagnetic wave, and *d* signifies the thickness of the samples.

3. Results and discussion

3.1. Morphology and structure characterization of material

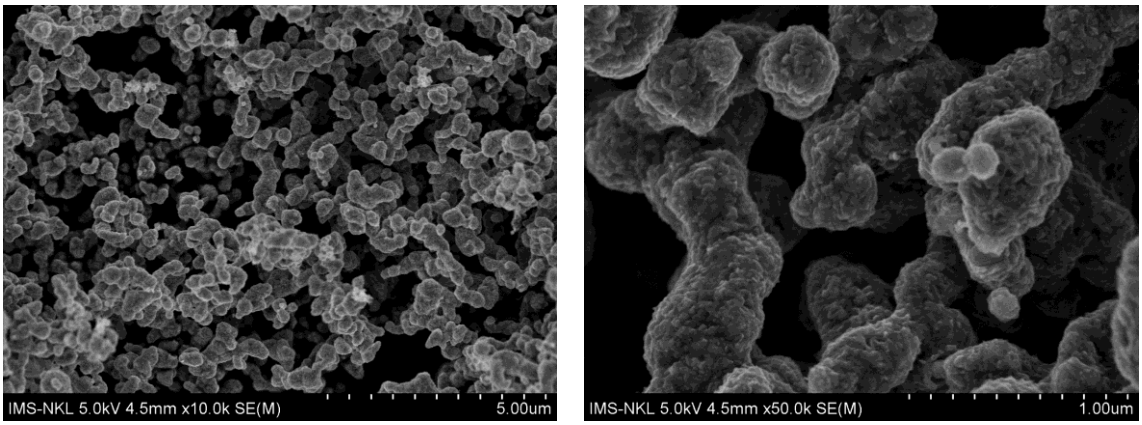

Fig. 1. SEM images of $NiCo_2O_4$ material.

The morphologies of the $NiCo_2O_4$ material was observed by SEM and shown in Fig. 1. The findings indicate that the nano-sized $NiCo_2O_4$ particles have led to the formation of tubular chains-like structural morphologies. These structures have a clear regular pattern, with spherical structures present at both ends. The spherical forms could be achieved by the presence of D-Glucose [10], whilst chains-like structures are likely favored by oxalate acid support [7]. The tubes have a diameter that varies between 400 and 500 nm. The tubes exhibit a consistent surface shape, which is defined by a well-organized pattern of $NiCo_2O_4$ particles at the nano-scale. Mechanisms such as electrical wave propagation inside the tubes, scattering and energy absorption inside the spheres and tubes, and complex energy scattering between the tubes, between the spheres, and between the sphere and the tube could also result from a hybridization of these two types of structures. Both the energy scattering capabilities and the energy dissipation of the $NiCo_2O_4$ material system are improved by these structural morphologies. Moreover, the surface roughness of the material layer enhances wave scattering and diffraction, resulting in increased energy loss due to the presence of more angles and surfaces for scattering. The intricate nature of the surface further amplifies the polarization capability at the material surface, hence facilitating wave absorption.

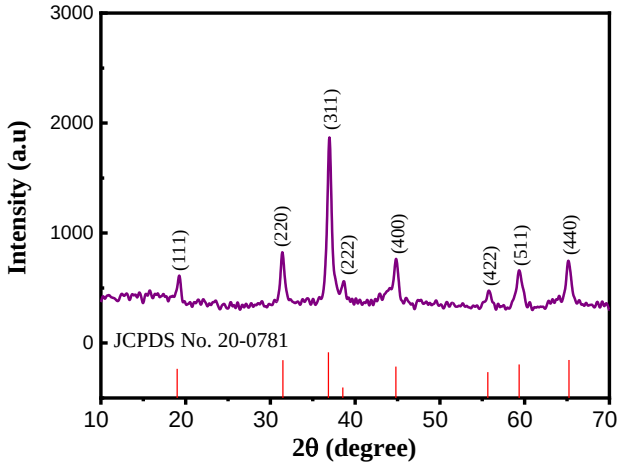

Fig. 2. XRD patterns of $NiCo_2O_4$ material.

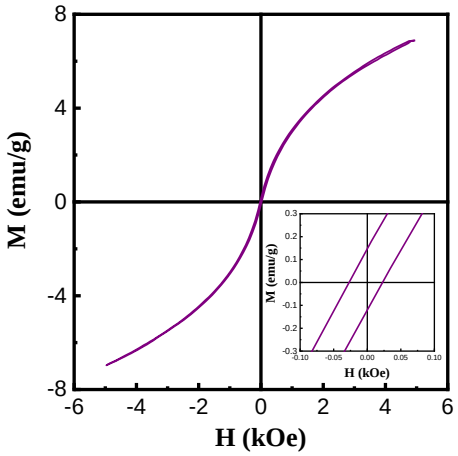

Fig. 3. Room temperature magnetic hysteresis loops of $NiCo_2O_4$.

In the XRD pattern of the $NiCo_2O_4$ sample (Fig. 2), characteristic peaks corresponding to planes (111), (220), (311), (400), (422), (511), and (440) were observed at 2θ angles of 18.9°, 31.1°, 36.7°, 44.6°, 55.4°, 59.1°, and 65.0°, respectively. These observations confirm that the $NiCo_2O_4$ material possesses a cubic spinel structure, consistent with the JCPDS No.20-0781 database [8]. Furthermore, the crystal sizes that correspond to the crystal plane positions (111), (220), (311), (400), (422), (511), and (440) were found to be 14.5, 14.6, 13.2, 12.4, 14.2, 12.6, and 14.5 nm, respectively, using the Scherrer formula. Thereby, the nano-sized $NiCo_2O_4$ particles have been found to have crystal diameters ranging from 12 to 15 nm.

The room temperature magnetization of $NiCo_2O_4$ was investigated, as depicted in Fig. 3. The material obtained using vibrating sample magnetometry (VSM) showed a remanence (M_r) of 0.15 emu/g and a coercive force (H_c) of 25 Oe, which are significantly near to zero. At 5 kOe, the magnetization value of the $NiCo_2O_4$ material was approximately 6.9 emu/g. The prompt reaction to external magnetic fields enhances the capacity to transfer electromagnetic waves through the tubes and establishes efficient routes for wave absorption.

3.2. Microwave absorption properties of material

Figure 4 illustrates the frequency-dependent curves of the complex permittivity and permeability of the $NiCo_2O_4$ sample.

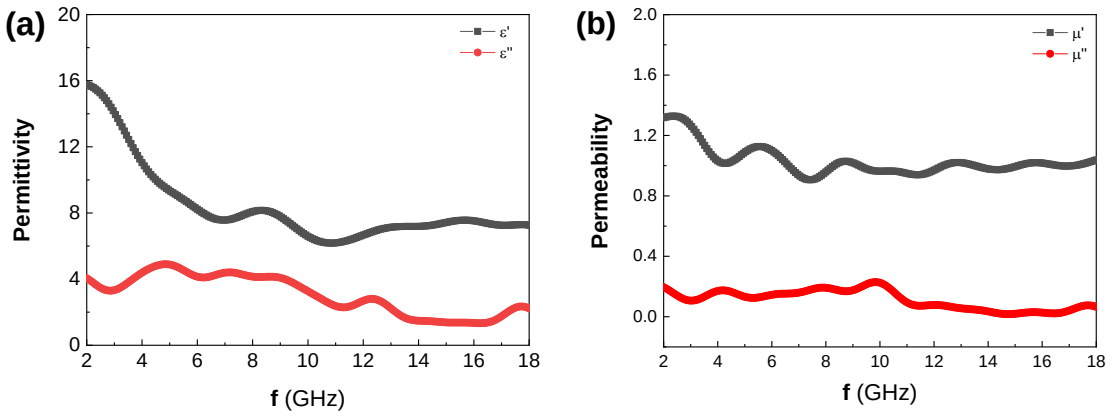

Fig. 4. The complex permittivity (a) and complex permeability (b) of $NiCo_2O_4$.

The real part of the complex permittivity decreases as frequency increases within the range of 2 - 18 GHz, which is consistent with the law of dipole polarization loss [12]. The value of ε' decreases rapidly in the low-frequency range (2 - 6 GHz), followed by minor changes at higher frequencies. The real part of the permittivity often reflects the ability to store electromagnetic waves within the structure. At low frequencies, the displacement of ions or electrons has sufficient time to keep pace with the changing external electric field, resulting in strong polarization and hence high permittivity. However, at high frequencies, particles cannot move fast enough to keep up with the rapidly changing electric field, reducing polarization and thus decreasing the permittivity [13]. In the case of nano-sized materials such as $NiCo_2O_4$, surface effects and particle structure also play significant roles. At low frequencies, surface effects and particle structure may cause stronger responses, leading to a decrease in permittivity [12].

A crucial measurement to determine the ability of a material to absorb energy within a particular frequency range, the imaginary component of the permittivity usually represents the material's attenuation coefficient for electromagnetic waves [14]. In free-electron theory, the imaginary part of the permittivity is frequency-dependent and is expressed as $\varepsilon'' = 1/(2\pi\varepsilon_0.\rho.f)$, where ρ is the material's resistivity and f is the electromagnetic wave's frequency [7]. The imaginary part of the dielectric constant exhibits a relatively minor decrease as frequency escalates within the range of 2 - 18 GHz for magnetic nano-materials. The minor decrease in the imaginary part of the dielectric constant is associated with energy loss due to the electromagnetic induction mechanism. This relates to the reorientation of polar molecules in a changing electric field. At low frequencies, molecules have sufficient time to reorient along the electric field, resulting in high energy loss due to the transfer of energy from the electric field to heat [9]. As the

frequency increases, the time for molecules to reorient becomes insufficient, reducing energy loss through this mechanism. The real part of the permeability also follows a decreasing trend at low frequency regions and shows minor variations at higher frequencies [15].

The real part of the permeability also follows a decreasing trend at low frequency regions and shows minor variations at higher frequencies. The phenomenon can be elucidated by considering loss processes that arise from natural resonance effects, specifically related to the rotation of magnetic moment vectors within a fluctuating magnetic field. The magnetic moments have plenty of time to realign in response to the magnetic field at low frequencies. This aligns them better with the field, increasing energy absorption and permeability. With increasing frequency, magnetic moments have less time to align. They cannot properly follow fast magnetic field changes, reducing energy absorption and actual permeability. As alignment time becomes more limited, the actual component of the permeability plateaus, with modest fluctuations at higher frequencies [11].

From 2 to 18 GHz, there are small changes in the imaginary component of the complex permeability. At higher frequencies, however, μ" becomes noticeably weaker. This lines up with two separate loss processes: low-frequency eddy current loss and high-frequency natural resonance loss.

The dielectric characteristics of the material are further investigated using Debye relaxation theory by examining the relationship between the real and imaginary parts of complex permittivity. The Cole-Cole equation may be used to perform one relaxing process, as shown below [16]:

$$\left(\varepsilon' - \frac{\varepsilon_s + \varepsilon_\infty}{2}\right)^2 + \varepsilon''^2 = \left(\frac{\varepsilon_s - \varepsilon_\infty}{2}\right)^2 \tag{3}$$

where ε_s, ε_∞ represent the static permittivity and the relative permittivity at the high-frequency limit, respectively.

The plot of ε' versus ε'' would be shown in a semicircle. Each semicircle represents Debye relaxation. Fig. 5a shows numerous semicircles, indicating multi-dielectric relaxation in the composite material. Distorted Cole-Cole semicircles also show defect and interfacial polarization, which increase dielectric loss [11]. $NiCo_2O_4$ heterogeneous surfaces may create more polarization centers under external electromagnetic fields, enhancing interfacial polarization and relevant relaxation.

The quantification of magnetic loss caused by eddy currents may be achieved by utilizing the coefficient C_0, which is defined as $C_0 = \mu''/(\mu'^2.f)$, where f indicates the frequency. Fig. 5b shows that the C_0 values of all samples display variations followed by a plateau, indicating the existence of natural resonance, exchange resonance, and eddy current losses. The C_0 curve has a consistent linear pattern with few rapid changes in frequency, indicating that the primary process at play is the dominance of eddy current loss [1].

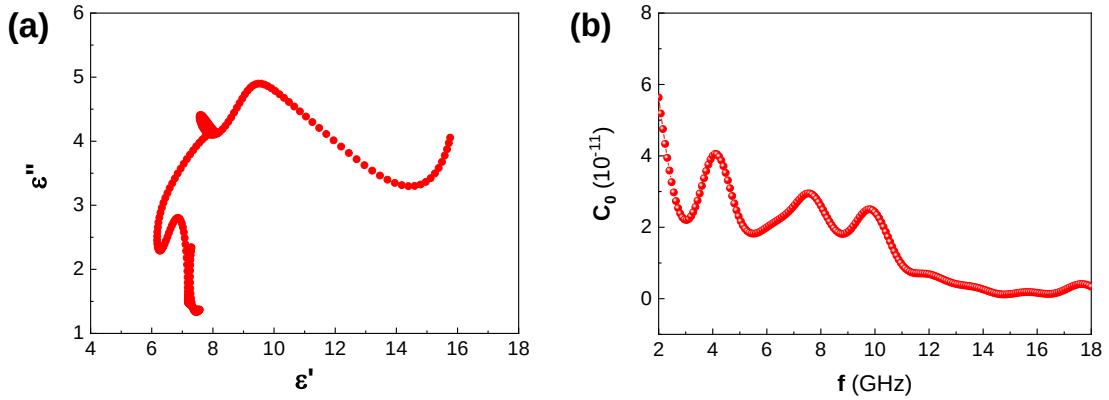

Fig. 5. The typical Cole-semicircle curve (a) and C_0 - f values (b) of $NiCo_2O_4$.

Furthermore, as shown by the following equations, the attenuation constant enhanced the microwave absorption capacities [9]:

$$\alpha = \frac{\sqrt{2}\pi f}{c}\sqrt{(\mu''\varepsilon'' - \mu'\varepsilon') + \sqrt{(\mu''\varepsilon'' - \mu'\varepsilon')^2 + (\mu'\varepsilon'' + \mu''\varepsilon')^2}} \quad (4)$$

where μ', μ'' are the real, imaginary part of complex permeability.

For $NiCo_2O_4$ material, the loss coefficient increases in the low-frequency range, then decreases at intermediate frequencies before rising again at high frequencies (Fig. 6a). At low frequencies, the natural resonance of the ferrite particles contributes to the increase in the loss coefficient. This enhancement may result from their high polarizability at low frequencies, leading to increased energy loss. As the frequency increases, the eddy current effect may diminish due to limitations imposed by the distribution and conductivity of the surface structure, as well as the interactions between particles. This leads to a decrease in the loss coefficient at intermediate frequencies, reflecting a reduction in effective electromagnetic interactions and energy scattering. At high frequencies, the resurgence of α can be attributed to the reinforcement of scattering and eddy current effects. Complex material structures, with well-dispersed $NiCo_2O_4$ particles, create numerous interfaces

and boundaries for wave scattering while stimulating the formation of stronger eddy currents at high frequencies. This, along with the polarizability at surfaces and complex interfaces, contributes to increased energy loss [10].

Figure 6b shows the Z_{in} impedance values for a 2.0 mm thick $NiCo_2O_4$ sample. Z_{in} values close to 1 in the 14.9 - 15.4 GHz frequency band of $NiCo_2O_4$ material indicate excellent impedance matching. By letting incoming electromagnetic waves pass through, the porous and hollow $NiCo_2O_4$ material enhances impedance matching [6].

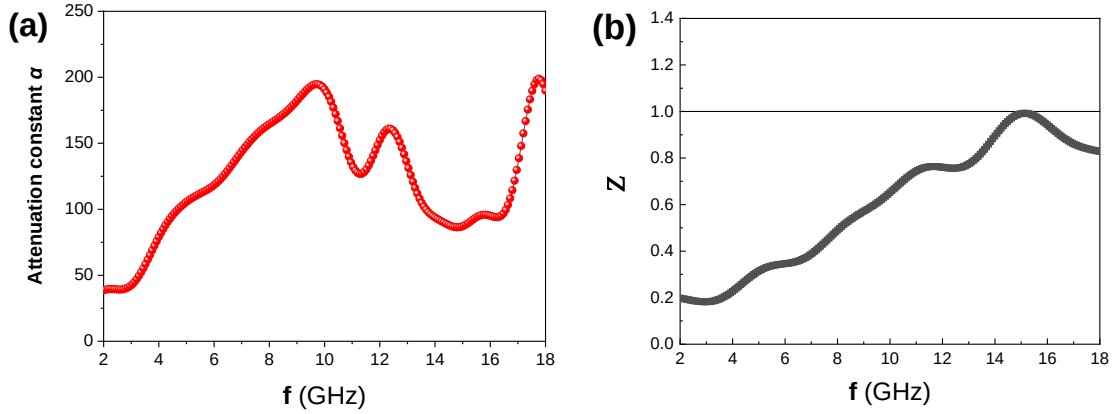

Fig. 6. Attenuation loss (a) and Z_{in} (b) of $NiCo_2O_4$ sample.

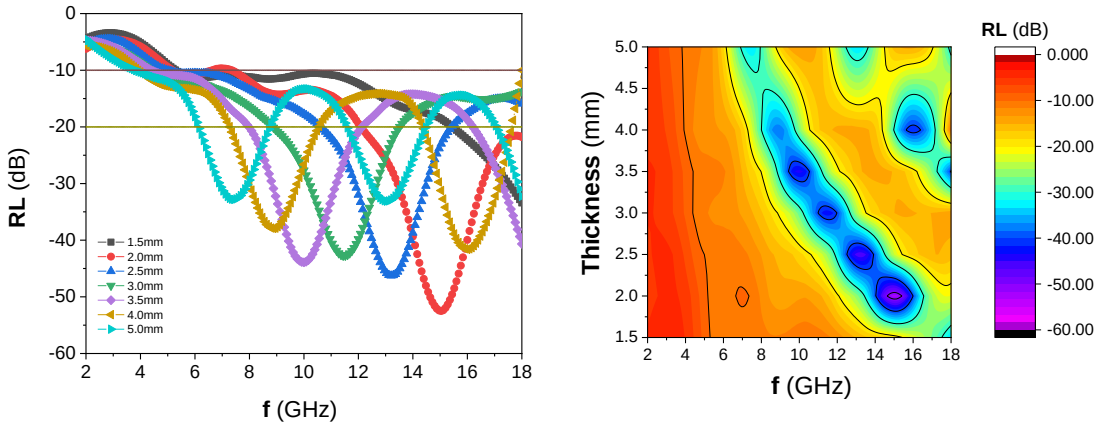

Fig. 7. Reflection loss of $NiCo_2O_4$ sample.

The RL measuring range is 2 - 18 GHz and 1.5 - 5.0 mm. For engineering uses involving microwave absorption, the material is suitable because to its sub-10 dB RL values, which dissipate almost 90% of entering EM waves. The range of RL values for $NiCo_2O_4$ material was presented in Fig. 7. Reduced RL_{min} is a function of increasing thickness. At 15 GHz, the $NiCo_2O_4$ material has the best reflection loss of -52.5 dB at a thickness of 2.0 mm. At this thickness, the effective absorption bandwidth is found to be

10.7 GHz. Also, at this thickness, across a broad frequency range (12.1 - 18 GHz), the reflection loss was consistently below -20 dB. A maximum effective range of 14.1 GHz is achieved by the $NiCo_2O_4$ material at a thickness of 5.0 mm.

Table 1. Comparison of the microwave absorption properties with other absorbers

Absorber	**RL_{min} (dB)**	**Bandwidth (GHz) (RL ≤ -10 dB)**	**Thickness (mm) Filled ratio (wt%)**	**Ref.**
$NiCo_2O_4$ urchin-like	-26.1	5.84	1.88 (50%)	[6]
$NiCo_2O_4$ hollow sphere-like	-37.0	4.64	1.9 (50%)	[10]
$NiCo_2O_4$ hollow sphere-like	-37.5	5.92	2.14 (80%)	[9]
$NiCo_2O_4$ sphere-like	-42.8	6.08	2.06 (50%)	[6]
$NiCo_2O_4$ column-like	-49.7	7.1	2.2 (50%)	[7]
$NiCo_2O_4$ flower-like	-50.3	4.0	3.0 (30%) 2.0 (30%)	[8]
$NiCo_2O_4$ nanochains-like	-52.5	10.7 14.1	2.0 (30%) 5.0 (30%)	**This work**

Table 1 presents a comparison of the microwave absorption characteristics of $NiCo_2O_4$ materials. Based on these comparisons, it can be concluded that the $NiCo_2O_4$ chains-like structure has exceptional microwave absorption capabilities, such as high reflection loss, wide absorption bandwidth, and a thin thickness.

The unique structure and composition of the $NiCo_2O_4$ chains-like material are related to its outstanding microwave absorption capability. First, the heterogeneity in the material's structure, particularly at the interfaces between $NiCo_2O_4$ particles, allows for the dispersion of electromagnetic waves [8]. The objective of optimizing the distribution of $NiCo_2O_4$ nano-particles is to increase the number of interfaces, which in turn improves energy scattering [9]. In addition, the interaction of particles with electromagnetic waves leads to different scattering and reflection processes, which cause varying levels of dispersion and consequent energy dissipation. Second, the presence of polarization within the $NiCo_2O_4$ particles and material interface structures, which results in the formation of chains and lattice structures, can lead to energy dissipation through both bipolar and ionic polarization. The purpose of engineering nano- and micro-structures is to increase polarization at these interfaces. The defects in the crystal structure of $NiCo_2O_4$ nano-particles can enhance energy absorption by inducing polarization at these specific defect

sites [10]. Finally, magnetic nanoparticles can absorb more energy at specific frequencies because they can naturally resonate at those same frequencies. High frequencies result in increased energy loss, which modifies the magnetic field as it passes through the material and produces eddy currents [11].

4. Conclusion

In this investigation, the $NiCo_2O_4$ chains-like structure displayed a remarkable microwave absorption performance. The tube diameter falls within the range of 400 - 500 nm. An optimal reflection loss value of -52.5 dB was achieved at 15 GHz with a sample thickness of 2.0 mm. The maximum effective bandwidth reached 14.1 GHz when the thickness was 5.0 mm. The primary electromagnetic energy loss mechanisms observed were multiple scattering, dipole polarization, natural resonance absorption, and eddy current losses. Consequently, the $NiCo_2O_4$ chains-like material prepared in this study is poised to exhibit exceptional electromagnetic wave absorption properties across the C, X, Ku bands.

Acknowledgements

The investigation was supported by Le Quy Don Technical University, Vietnam.

References

[1] P. T. Tho, C. T. A. Xuan, N. Tran, …, B. W. Lee, "Ultra-wide effective absorption bandwidth of Cu, Co, and Ti co-doped $SrFe_{12}O_{19}$ hexaferrite," *Ceram. Int.*, Vol. 48 (19), pp. 27409-27419, 2022. DOI: 10.1016/j.ceramint.2022.05.389

[2] C. T. A. Xuan, P. T. Tho, T. Q. Dat, …, N. Tran, "Development of high-efficiency microwave absorption properties of $La_{1.5}Sr_{0.5}NiO_4$ and $SrFe_{12}O_{19}$-based materials composites," *Surf. Interfaces*, Vol. 39, 2023, 102890. DOI: 10.1016/j.surfin.2023.102890

[3] H. Pang, Y. Duan, L. Huang, …, X. Liu, "Research advances in composition, structure and mechanisms of microwave absorbing materials," *Compos. B. Eng.*, Vol. 224, 2021, 109173. DOI: 10.1016/j.compositesb.2021.109173

[4] T. Q. Dat, N. T. Ha, N. V. Tung, and P. V. Thin, "Microwave absorption performances of copper/nickel ferrite@fiber polyaniline," *Journal of Science and Techique*, Vol. 16, No. 02, pp. 5-13, 2021. DOI: 10.56651/lqdtu.jst.v16.n02.262

[5] J. Y. Yusuf, H. Soleiman, N. Yahya, …, F. A. Wahaab, "Recent advances and prospect of cobalt based microwave absorbing materials", *Ceram. Int.*, Vol. 46 (17), pp. 26466-26485, 2020. DOI: 10.1016/j.ceramint. 2020.07.244

[6] H. Wu, M. Qin, and L. Zhang, "$NiCo_2O_4$ constructed by different dimensions of building blocks with superior electromagnetic wave absorption performance", *Compos. Part B-Eng.*, Vol. 182, 2020, 107620. DOI: 10.1016/j.compositesb.2019.107620

[7] Q. Chang, H. Liang, B. Shi, and H. Wu, "Sodium oxalate-induced hydrothermal synthesis of wood-texture column-like $NiCo_2O_4$ with broad bandwidth electromagnetic wave absorption performance", *J. Colloid Interface Sci.*, Vol. 600, pp. 49-57, 2021. DOI: 10.1016/j.jcis.2021.05.019

[8] X. Su, J. Wang, X. Zhang, …, B. Zhang, "Design of controlled-morphology $NiCo_2O_4$ with tunable and excellent microwave absorption performance," *Ceram. Int.*, Vol. 46 (6), pp. 7833-7841, 2020. DOI: 10.1016/j.ceramint.2019.12.002

[9] M. Qin, L. Zhang, X. Zhao, and H. Wu, "Defect induced polarization loss in multishelled spinel hollow spheres for electromagnetic wave absorption application", *Adv. Sci.*, Vol. 8, 2021, 2004640. DOI: 10.1002/advs.202004640

[10] M. Qin, L. Zhang, and H. Wu, "Dual-template hydrothermal synthesis of multichannel porous $NiCo_2O_4$ hollow spheres as high-performance electromagnetic wave absorber", *Appl. Surf. Sci.*, Vol. 515, 2020, 146132. DOI: 10.1016/j.apsusc.2020.146132

[11] T. Q. Dat, N. T. Ha, and D. Q. Hung, "Reduced graphene oxide-$Cu_{0.5}Ni_{0.5}Fe_2O_4$-Polyaniline nanocomposite: Preparation, characterization and microwave absorption properties", *J. Electron. Mater.*, Vol. 46, pp. 3707-3713, 2017. DOI: 10.1007/s11664-017-5386-z

[12] N. V. Tung, T. Q. Dat, N. T. Ha, N. T. Nam, and D. Q. Hung, "Synthesis of reduced graphene oxide - $Mn_{0.8}Zn_{0.2}Fe_2O_4$ - porous polyaniline nanocomposite materials for effective microwave absorption in X-band," *Journal of Science and Techique*, Vol. 15, No. 5, pp. 13-23, 2020. DOI: 10.56651/lqdtu.jst.v15.n05.81

[13] M. Qin, H. Liang, X. Zhao, and H. Wu, "Filter paper templated onedimensional NiO/$NiCo_2O_4$ microrod with wideband electromagnetic wave absorption capacity," *J. Colloid Interface Sci.*, Vol. 566, pp. 347-356, 2020. DOI: 10.1016/j.jcis.2020.01.114

[14] H. Wang and J. Cui, "Preparation of $NiCo_2O_4$ with different morphologies and its effect on absorbing properties," *Mater. Lett.*, Vol. 236, pp. 465-467, 2019. DOI: 10.1016/j.matlet.2018.10.164

[15] T. Q. Dat, N. V. Tuan, N. V. Tung, and P. V. Thin, "Facile synthesis of MoS_2 nanomaterial as a promising microwave absorber," *Journal of Science and Techique*, Vol. 17, No. 05, pp. 5-15, 2022. DOI: 10.56651/lqdtu.jst.v17.n05.526

[16] P. V. Thin, L. D. Vi, N. V. Tuan, …, T. Q. Dat, "Synthesis of Fe_3O_4 nanoparticles grown on rice husk waste-derived porous carbon for high-efficiency microwave absorption," *Journal of Science and Technique*, Vol. 1, No. 02, pp. 27-39, 2023. DOI: 10.56651/lqdtu.jst.v1.n02.692.pce

TỔNG HỢP VẬT LIỆU CHUỖI NANO $NiCo_2O_4$ VỚI ĐẶC TÍNH HẤP THỤ VI SÓNG HIỆU NĂNG

Trần Quang Đạt[1], Nguyễn Tuấn Linh[1], Nguyễn Văn Cường[1]

[1]*Khoa Hóa - Lý kỹ thuật, Trường Đại học Kỹ thuật Lê Quý Đôn, Hà Nội, Việt Nam*

Tóm tắt: Vật liệu $NiCo_2O_4$ dạng chuỗi nano được tổng hợp thông qua phương pháp thủy nhiệt sử dụng D-glucose làm chất đệm để tạo điều kiện cho hấp thụ sóng vi sóng trên dải tần từ 2 đến 18 GHz. Từ đó, các phương pháp phân tích khác nhau đã được thực hiện để nghiên cứu cấu trúc, cấu trúc vi mô, tính từ và đặc trưng điện từ của vật liệu. Nhờ sử dụng axit oxalic và D-glucose, cấu trúc chuỗi bao gồm các hạt nano cầu (400 - 600 nm) đã được tổng hợp thành công. Vật liệu $NiCo_2O_4$ có cấu trúc tinh thể đơn pha và có tổn hao phản xạ (RL) thấp hơn -20 dB lên đến 5,9 GHz trong dải tần Ku (12 - 18 GHz), ở mẫu có bề dày 2,0 mm. Đáng chú ý, tổn hao phản xạ tối ưu đạt đến -52,5 dB tại 15 GHz cho các mẫu với độ dày là 2,0 mm, trong khi băng thông hiệu quả rộng nhất kéo dài lên đến 14,1 GHz cho các mẫu với độ dày là 5,0 mm. Hiệu suất hấp thụ vi sóng vượt trội của vật liệu $NiCo_2O_4$ dạng chuỗi nano là nhờ sự tương tác tương hỗ giữa các đặc tính điện môi và từ tính của chúng, tạo điều kiện cho khả năng phối hợp trở kháng tối ưu. Những kết quả này chỉ ra rằng các loại bột dạng chuỗi $NiCo_2O_4$ có nhiều triển vọng làm vật liệu hấp thụ vi sóng.

Từ khóa: *$NiCo_2O_4$; xốp; thủy nhiệt; hấp thụ vi sóng.*

Received: 06/04/2024; Revised: 22/04/2024; Accepted for publication: 02/05/2024

❑